

Insights into the neurochemical signature of the Innervation of Beige Fat



Aneta Stefanidis^{1,2}, Nicole M. Wiedmann³, Sonika Tyagi⁴, Andrew M. Allen⁵, Matthew J. Watt^{1,2}, Brian J. Oldfield^{1,2,*}

ABSTRACT

Objective: The potential for brown adipose tissue (BAT) to be targeted as a therapeutic option to combat obesity has been heightened by the discovery of a brown-like form of inducible “beige” adipose tissue in white fat which has overlapping structural and functional properties to “classical” BAT. The likelihood that both beige and brown fat are recruited functionally by neural mechanisms, taken together with the lack of a detailed understanding of the nature of changes in the nervous system when white adipose tissue (WAT) is transformed to brown, provides the impetus for this study. Here, we aim to identify whether there is a shift in the gene expression profile in neurons directly innervating inguinal white adipose tissue (iWAT) that has undergone “beiging” to a signature that is more similar to neurons projecting to BAT.

Methods: Two groups of rats, one housed at thermoneutrality (27 °C) and the other exposed to cold (8 °C) for 7 days, were killed, and their T13/L1 ganglia, stellate ganglion (T1/T2), or superior cervical ganglion (SCG, C2/3) removed. This approach yielded ganglia containing neurons that innervate either beiged white fat (8 °C for 7 days), inguinal WAT (27 °C for 7 days), BAT (both 27 °C and 8 °C for 7 days) or non-WAT (8 °C for 7 days), the latter included to isolate changes in gene expression that were more aligned with a response to cold exposure than the transformation of white to beige adipocytes. Bioinformatics analyses of RNA sequencing data was performed followed by Ingenuity Pathway Analysis (IPA) to determine differential gene expression and recruitment of biosynthetic pathways.

Results: When iWAT is “beiged” there is a significant shift in the gene expression profile of neurons in sympathetic ganglia (T13/L1) innervating this depot toward a gene neurochemical signature that is similar to the stellate ganglion projecting to BAT. Bioinformatics analyses of “beiging” related genes revealed upregulation of genes encoding neuropeptides proopiomelanocortin (POMC) and calcitonin-gene related peptide (CGRP) within ganglionic neurons. Treatment of differentiated 3T3L1 adipocytes with α MSH, one of the products cleaved from POMC, results in an elevation in lipolysis and the beiging of these cells as indicated by changes in gene expression markers of browning (*Ucp1* and *Ppargc1a*).

Conclusion: These data indicate that, coincident with beiging, there is a shift toward a “brown-like” neurochemical signature of postganglionic neurons projecting to inguinal white fat, an increased expression of POMC, and, consistent with a causative role for this prohormone in beiging, an α MSH-mediated increase in beige gene markers in isolated adipocytes.

© 2018 The Authors. Published by Elsevier GmbH. This is an open access article under the CC BY-NC-ND license (<http://creativecommons.org/licenses/by-nc-nd/4.0/>).

Keywords Beige fat; RNA sequencing; Brown adipose tissue; Thermogenesis

1. INTRODUCTION

The rejuvenation of interest in BAT in the last decade has been driven by two major revelations. The first was the realization that brown fat exists in adult humans based on identification of supraclavicular uptake of 18F-FDG co-registered with PET/CT imaging [1,2] and publication of the first retrospective analyses of 18F-FDG PET/CT scans [3], which preceded the three landmark publications in 2009 that demonstrated that BAT is not only present in adult humans [4–6] but exists in amounts inversely proportional to BMI and fat mass [6]. The

second was the discovery of an inducible form of brown-like fat, so-called “brite” or “beige” fat. While the nomenclature has implications that relate to its functional origins with the term “brite” referring to the derivation of brown from white fat [7] and “beige” being consistent with a unique progenitor [8], the term beige will be used here. It is striking that in its short history, beige fat has been at the center of several controversies. As alluded to above, its embryological origins have been described differently, and these views are supported by what appear to be equally compelling data; so, these disparate perspectives remain embedded in our understanding of BAT biology. Subcutaneous

¹Department of Physiology, Monash University, Clayton, Victoria, Australia ²Metabolism, Diabetes and Obesity Program, Biomedicine Discovery Institute, Monash University, Clayton, Victoria, Australia ³Department of Anatomy and Neuroscience, University of Melbourne, Parkville, Victoria, Australia ⁴Monash Bioinformatics Platform, Monash University, Clayton, Victoria, Australia ⁵Department of Physiology, University of Melbourne, Parkville, Victoria, Australia

*Corresponding author. Department of Physiology, Monash University, Clayton, Australia. E-mail: brian.oldfield@monash.edu (B.J. Oldfield).

Abbreviations: α MSH, alpha melanocyte stimulating hormone; BAT, brown adipose tissue; BMI, body mass index; CGRP, Calcitonin gene-related peptide; CT, computed tomography; FDR, false discovery rate; IPA, Ingenuity Pathway Analysis; iBAT, interscapular brown adipose tissue; iWAT, inguinal white adipose tissue; PCA, principal component analysis; PET, positron emission tomography; POMC, Pro-opiomelanocortin; RNA-Seq, RNA Sequencing; SCG, Superior cervical ganglion; TH, tyrosine hydroxylase; UCP1, Uncoupling Protein 1; WAT, white adipose tissue

Received December 26, 2017 • Revision received January 17, 2018 • Accepted January 30, 2018 • Available online 10 February 2018

<https://doi.org/10.1016/j.molmet.2018.01.024>

WAT, particularly in the inguinal depot is shown to undergo a process of “beiging” in which thermogenic, mitochondrial rich, UCP1-expressing multilocular cells develop within white adipocytes [9]. On one hand, these have been described as arising from the transformation of mature white adipocytes to brown-like/beige adipocytes in a reversible manner driven primarily, but not exclusively, by elevated levels of noradrenergic stimulation [10]. The equally compelling alternative view is that beige adipocytes are derived under a range of conditions from dedicated beige precursors, identified by a characteristic complement of genes, that are already present in the tissue during development [11,12]. More recently, another form of beige fat has been identified that is capable of thermogenic activity without what has been thought of as its essential thermogenic ingredient, UCP1 [13]. In addition to conflicting views about its origins, the question of the extent to which brown-like fat is represented in adult humans as beige or “classical” brown fat remains unresolved [14–18].

Irrespective of the details of the origins of beige fat, whether it be by transformation from mature white adipocytes or derivation from dedicated precursors, the fact remains that there is evidence that it contributes in a functionally appropriate way to metabolic improvement under various conditions in both rodents and humans [19–21]. The question which forms the basis of this study is the following. How is it that WAT, which is supported in its primary functions of lipid storage and lipolysis by integrated neural circuits, becomes functionally more aligned with energy expenditure when mammals are exposed to cold and white fat is turned to beige? At face value, this transition between fat types would necessarily involve input from different central circuits recruited by very different sensory modalities controlling such disparate functions. A well-established tenet of the organization and function of the autonomic nervous system is that the sympathetic innervation of particular end organs is associated with a characteristic chemical profile which is most pronounced in neurons of the paravertebral ganglion innervating that structure [22–24]. As such subpopulations of neurons innervating different target tissues can express unique combinations of neurotransmitters, neuropeptides, ion channels and receptors and form a “neurochemical signature” which, if not unique, is characteristic of that neuron to target organ connection [23–27].

In the case of the postganglionic innervation of the iBAT and iWAT, these populations of neurons are contained within the stellate ganglion and T13/L1 sympathetic ganglia, respectively. The neurochemical profile of the stellate ganglion neurons innervating either blood vessels or brown adipocytes has been previously established; neurons projecting to blood vessels contain TH and neuropeptide Y but not calbindin [28], whereas viral tracing studies have identified the neurochemical signature of neurons projecting to BAT as containing TH and calbindin but rarely neuropeptide Y [29]. While the chemical code of neurons in the T13/L1 ganglion projecting to iWAT is unknown, it is likely that, coincident with the transition from iWAT to beige fat after exposure to cold or otherwise elevated β -adrenoceptor activation, there is a corresponding shift in the neurochemical coding of neurons innervating that fat depot.

In the present experiments, we have utilized cold exposure to generate a brown-like phenotype in the iWAT of rats. We hypothesize that when the function of iWAT changes from energy storing to energy burning with cold exposure, that the neurochemical phenotype of ganglionic neurons within the T13/L1 ganglia will shift towards the phenotype seen within the BAT-projecting neurons in the stellate ganglion. In order to identify the changes in the neurochemical profile of sympathetic ganglia, we have utilized next generation RNA sequencing (RNA-Seq) to identify differential gene expression. This method allows us to describe the nature of the innervation of beighed iWAT and compare it to that of neurons projecting to iWAT and iBAT at thermoneutrality.

2. METHODS

2.1. Animals and housing

Male Sprague–Dawley rats were obtained from Monash Animal Services (Clayton, VIC, Australia). Rats ($n = 17$) weighing 200–220 g were housed individually under standard housing conditions on a 12 h:12 h light/dark cycle, and were provided *ad libitum* access to water and standard laboratory chow (12% kcal from lipids). Rats were either housed in a thermoneutral environment (27 °C) or underwent exposure to cold (8 °C) for 7 days. All experiments were approved by the Monash University Animal Research Platform Ethics Committee (MARP/2013/099).

2.2. Tissue collection

Rats were deeply anesthetized with an injection of pentobarbitone sodium (100 mg/kg, i.p) and then flushed with RNase-free 0.9% physiological saline. Stellate ganglia (T1/T2), T13/L1 ganglia, and superior cervical ganglia (SCG) were dissected under microscopic guidance from a ventral aspect following identification of the sympathetic chain. Individual ganglia were immediately stored in RNase Later (Thermo Scientific, Wilmington, DE, USA) before RNA extraction.

2.3. RNA extraction

RNA was extracted using the RNeasy Mini Kit (Qiagen, VIC, Australia) and DNA fragments removed with the RNase-Free DNase Set (Qiagen, VIC, Australia) from the stellate ganglion, T13/L1 ganglia and SCG.

2.4. RNA-sequencing and bioinformatics analysis

RNA was transcribed and amplified via Ovation RNA-Seq system V2 and Ovation® Ultralow Library Systems V2 (NuGEN Technologies). Sequence data was generated by the Medical Genomics Facility at Monash Health Translation Precinct (MHTP). Raw reads from the RNA-Seq libraries were quality checked using the Fastqc tool (v0.11.5). RNA-Seq libraries were mapped to the Rat genome (Ensembl version Rnor_6.0) using the STAR software v2.5.2 [30], with the number of reads mapped to each gene calculated using the featureCounts tool from the Subread package [31]. Mapping statistics were summarized using MultiQC tool [32]. Stellate and T13/L1 ganglia samples yielded 19–23 million reads that uniquely mapped to the genome, of which 14–20 million reads uniquely mapped to the known genes. SCG samples generated 40–64 million reads which uniquely mapped to the genome, of which 33–52 million uniquely mapped to the known genes. This difference in this sequencing depth was accounted for during the normalization of the datasets.

Differential expression analysis was carried out using edgeR [33] along with the RUVseq [34] to remove unwanted noise in the data. The upper quartile normalization method was used and PCA plots showed expected clustering of samples into groups (Supplementary Figure 1). Significant differentially expressed genes were selected using log-fold-change of ± 1 and FDR cut-off of 0.05 and were used for performing pathway enrichment analysis using IPA (Qiagen Bioinformatics, Redwood City, CA).

2.5. Impact of neuropeptides (CGRP and α MSH) on markers of browning

Cell culture studies: 3T3L1 preadipocytes were cultured in high glucose Dulbecco's modified Eagle's medium DMEM (DMEM + GlutaMAX) (Gibco, Life Technologies) supplemented with 10% (v/v) FBS (Gibco, Life Technologies) and 1% penicillin and streptomycin in a humidified 5% CO₂ atmosphere. The day after cells reached confluence, cells were differentiated using 3-isobutyl-1-methylxanthine (500 μ M; Sigma), dexamethasone (5 μ M; Sigma, St.

Louis, MO, U.S.A.), biotin (0.1 $\mu\text{g}/\text{mL}$) and insulin (0.05U/mL) for 3 days, followed by culture with insulin (0.05U/mL) in DMEM containing 10% FBS and 1% antibiotics. Prior to drug treatment, insulin was removed from the media for 24 h. On the experimental day, increasing concentrations CGRP (0, 10^{-12} , 10^{-9} , 10^{-6} M; Bachem, Bubendorf, Switzerland) or αMSH (0, 10^{-13} , 10^{-10} , 10^{-7} M; Tocris Bioscience, Bristol, United Kingdom) were applied to the mature adipocytes for 6 h. Cells were then washed with ice-cold PBS and collected for the assessment of gene expression.

Gene expression analysis using quantitative real-time PCR. Total RNA was extracted from the harvested cells using Trizol reagent (Thermo Scientific, Wilmington, DE, USA) and quantity determined using a NanoDrop (Thermo Scientific, Wilmington, DE, USA). RNA was reverse transcribed into cDNA (iScript Reverse Transcription Supermix for RT-qPCR, Bio-rad Laboratories, Hercules, CA, USA), and gene expression was determined by quantitative real-time PCR using the TaqMan Universal PCR Master Mix and TaqMan Gene Expression Assays (Applied Biosystems, Foster City, CA) for *Ucp1* (Mm01244861_m1) and *18S* (Mm03928990_g1) and SYBR Green PCR Master Mix (QuantiNova SYBR Green RT-PCR Master Mix) for *Ppargc1a* (from M. Swarbrick) and *18S* (from R. Stark). Amplifications were performed using a Real Plex4 Mastercycler (Eppendorf) for Taqman assays and CFX384 Touch Real-Time PCR Detection System (Bio-Rad, Gladesville, New South Wales, Australia) for SYBR green assays. Relative gene expression was calculated using the $2^{-\Delta\Delta\text{CT}}$ method.

3. RESULTS

3.1. Gene expression profiles of neurons in the T13/L1 ganglia innervating iWAT and beiged iWAT — comparison with stellate ganglion projections to iBAT

In order to assess whether there is a characteristic gene expression profile in sympathetic ganglionic neurons that innervate iWAT that shifts as this fat depot becomes beige under conditions of cold, RNA-Seq was undertaken comparing levels of gene expression in T13/L1 and stellate ganglia either at thermoneutrality (27 °C) or following 7 days cold (8 °C) exposure. The T13/L1 ganglia and the stellate ganglion are the primary ganglia directing post-ganglionic fibers to iWAT and iBAT, respectively. The basic comparisons undertaken in this gene analysis were between neurons innervating iWAT versus iBAT, i.e. T13/L1 versus stellate ganglia at 27 °C [Table 1(A)]; iWAT versus beiged iWAT, i.e. T13/L1 ganglia at 27 °C and 8 °C [Table 1(B)]; beiged iWAT versus iBAT, i.e. T13/L1 ganglia at 8 °C and stellate ganglion at 8 °C [Table 1(D)]. In the latter case, the analysis of stellate ganglion at 8 °C was included to compensate for any changes in the innervation of iBAT coincident with cooling. The final comparison of beiged iWAT versus ganglion deemed unlikely to have a significant projection to WAT, i.e. T13/L1 ganglia at 8 °C and superior cervical ganglia (SCG) at 8 °C [Table 1(E)], was also included to control for effects on gene expression in sympathetic ganglia that were solely related to cooling. All comparisons and the rationale for their inclusion in the analyses are summarized in Table 1.

3.2. Changes in gene expression between neurons in ganglia projecting to iWAT and iBAT under thermoneutral and cold conditions

Fold changes, which represent the changes in gene expression between two variables, in this case ganglia and/or temperature, are shown in Figure 1 both as “pie charts” and more conventionally as “smear plots”. The latter depicts gene fold change plotted against statistical significance value. When rats were housed at 27 °C, gene

expression in T13/L1 ganglia and stellate ganglia were different with 3227 (1713 upregulated [12.6%] and 1514 down-regulated [11.1%]) differentially expressed genes reflecting the functional differences in the target fat depots at thermoneutrality (Figure 1A). Comparing T13/L1 ganglia from rats housed under the two different temperature conditions (27 °C and 8 °C), there were 3716 (2922 upregulated [21.4%] and 794 down-regulated [5.8%]) differentially expressed genes, consistent with a significant shift ($\text{FDR} < 0.05$) in gene expression in the neural input to iWAT coincident with being at cold temperatures (Figure 1B). By comparison, there was a smaller shift of 2211 differentially expressed (1723 upregulated [12.6%] and 488 downregulated [3.6%]) genes in the stellate ganglion under the two temperature conditions (Figure 1C).

One of the most pertinent comparisons was that between T13/L1 and stellate ganglia at 8 °C. The results showed that after cold exposure, there was a reduction in the differentially expressed genes from 3227 at 27 °C to 741 (494 upregulated [3.6%] and 247 downregulated [1.8%]) at 8 °C (Figure 1D), indicating that with being, there was a corresponding shift in the gene expression of neurons in T13/L1 to become more “brown-like” in their gene expression profile.

In order to further isolate possible changes in gene expression as a result of a whole body physiological response to cold exposure, T13/L1 and stellate ganglion were compared to the SCG, a ganglion with sympathetic neurons innervating structures in the head and neck and considered to have little involvement in the innervation of major adipose tissue depots. When rats were housed at 8 °C, the gene expression profile of SCG compared to that in either T13/L1 or stellate ganglia was significantly different, with 4284 (1142 upregulated [8.1%] and 3142 downregulated [22.4%]) genes differentially expressed in T13/L1 and 3729 (798 upregulated [5.7%] and 2931 downregulated [20.9%]) genes differentially expressed in the stellate (Figure 1E,F). These data indicate that under conditions of cold, there are significant differences in gene expression between these ganglia showing that the results above (Figure 1A) are not a generalized response to cold.

3.3. Candidates involved in the innervation of beige adipose tissue based on fold change in specific genes and gene pathways

3.3.1. Rationale for screening approach

Under conditions of cold, comparison of shifts in gene expression profiles in the stellate and T13/L1 ganglia relative to those in the SCG, which has neuronal projections directed to the head and upper neck with a paucity of input to adipose tissue depots, allows an assessment of differentially expressed genes that are likely to be due to being rather than a generalized response to cooling. The rationale for this comparison is as follows: Genes that are specifically associated with “being” need to be both i) differentially expressed in T13/L1 when comparisons are made between 27 °C and 8 °C and ii) differentially expressed when comparisons are made between T13/L1 and SCG at 8 °C. This overlap represents the set of genes that are changed in T13/L1 but are not similarly expressed in the SCG. Those genes that are similarly expressed in the T13/L1 and SCG at 8 °C would be reasonably designated as responding to cold alone (see Figure 2).

3.3.2. Whole genome sequencing

High-throughput RNA-Seq enabled the identification and measurement of transcript expression in response to cold exposure. Using the approach described above, we compared the gene expression profiles between the T13/L1 ganglia and SCG at 8 °C. Further analysis revealed 3502 significantly differentially regulated genes ($\text{FDR} \leq 0.05$) in the

T13/L1 ganglia that were independent of the cold exposure and occurred concomitantly with the being of iWAT. The 40 most variable of these genes (20 upregulated and 20 downregulated) are listed in Table 2. It was interesting to note the presence of *Ucp1* (8.03 logFC) and *Cidea* (6.28 logFC) in this category; these genes were significantly up-regulated in T13/L1, and these changes are concomitant with the being of iWAT.

3.3.3. Screening known neuropeptides/neuromodulators in paravertebral ganglia

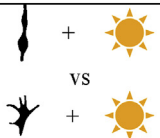

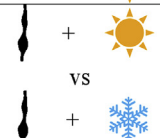

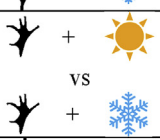
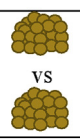
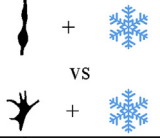

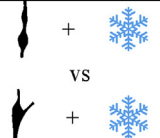

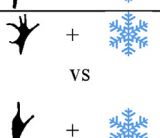
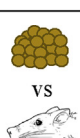
Shifts in gene expressions for known neuropeptides and neurotransmitters present within sympathetic ganglia were established (Table 3). The two genes that displayed the greatest significant ($FDR \leq 0.05$) shift in expression were those encoding calcitonin gene-related peptide (CGRP, *Calca*, up-regulated 2.03 logFC) and proenkephalin (*Penk*, up-regulated 1.90 logFC) (Table 3). There was also a 2- and 1-fold increase in the expression of *Tac1* and *Nos1*, the genes encoding

Substance P and Nitric Oxide Synthase 1, respectively. The fold changes in these four peptides were further reflected in the total number of reads determined through RNA-Seq, showing significant elevation after cold exposure (Figure 3).




3.3.4. Analysis of identified biosynthetic pathways by IPA

In addition to the unbiased approaches to the analyses of shifts in gene expression, analyses of canonical pathways were carried out by subjecting the pre-filtered list of “being” related differentially expressed genes within the T13/L1 ganglia with a $FDR \leq 0.05$ to IPA. The significance score was expressed as the negative logarithm of the P value, indicating the likelihood that the focus genes were assembled into a pathway. IPA identified 476 altered pathways in the T13/L1 ganglia when assessing genes that are associated with the being of iWAT. Interestingly, there was an overrepresentation of genes associated with mitochondrial dysfunction, oxidative phosphorylation, fatty acid oxidation, and insulin receptor signaling following cold-induced

Table 1 — Differential gene expression comparisons used for RNA-Seq data and rationale for their inclusion.

Comparison of ganglia	Comparison of adipose tissue depots	Rationale
A  + vs +	 vs +	Establishes the difference in gene expression between neurons projecting to iWAT and iBAT at thermoneutrality.
B  + vs +	 vs +	Identifies if there is a shift in gene expression profile in neurons projecting to iWAT when it undergoes being under cold conditions.
C  + vs +	 vs +	Determines the effect of cooling on gene expression profile in the stellate ganglion when the target organ (BAT) does not change its phenotype.
D  + vs +	 vs +	Establishes whether cold exposure can induce changes in gene expression in T13/L1 to become more “brown-like” ie similar to stellate ganglion projections to iBAT
E  + vs +	 vs +	Allows the identification of differentially expressed genes that may be the result of a whole-body response to cold
F  + vs +	 vs +	Allows the identification of differentially expressed genes that may be the result of a whole-body response to cold

Key terms and symbols: iWAT, inguinal adipose tissue; iBAT, interscapular brown adipose

tissue; , stellate ganglion; , T13/L1 ganglia; , superior cervical ganglion (SCG)

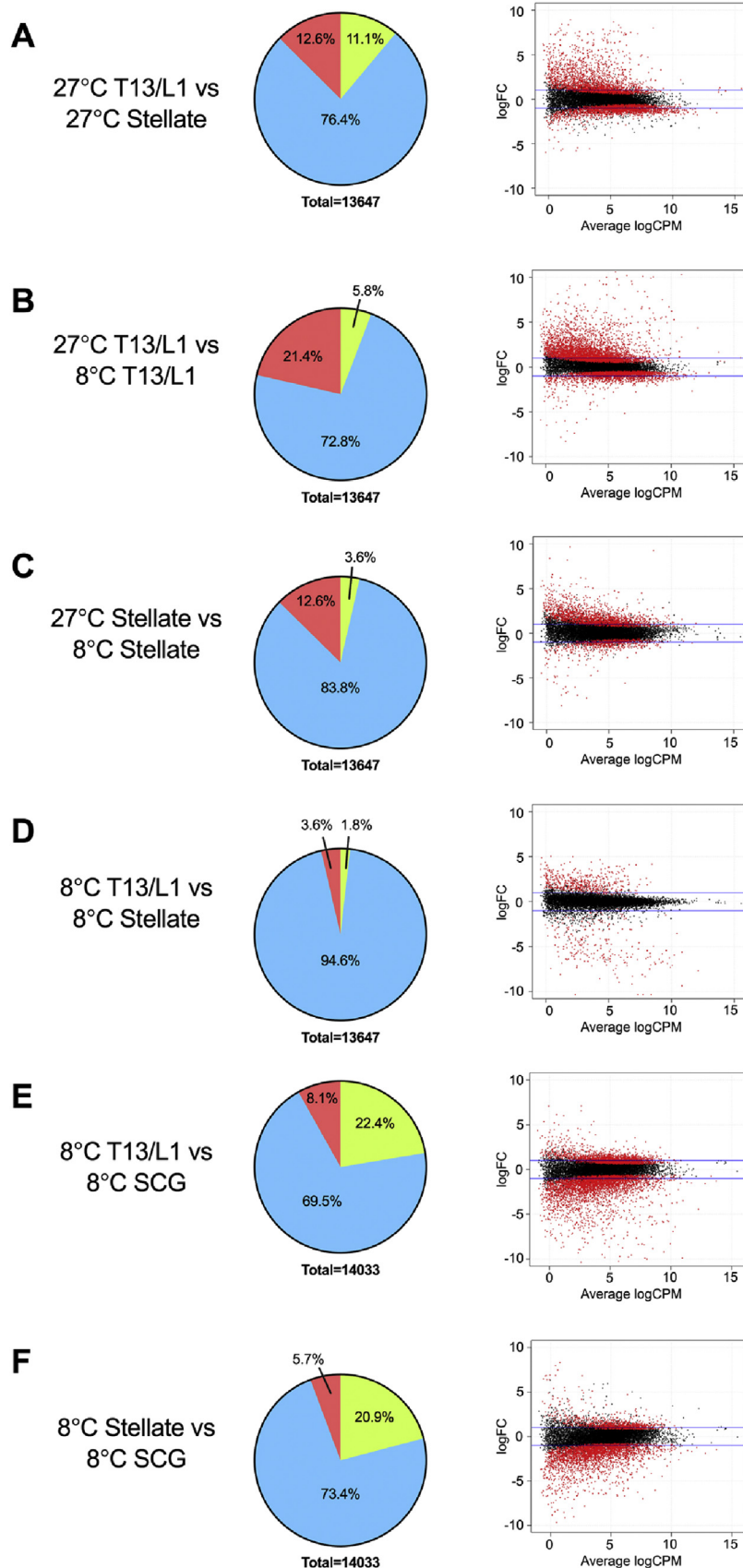


Figure 1: Pie charts (left column) showing the percentage of differential gene expression with a fold change greater than \log_2 (FDR ≤ 0.05) and smear plots (right column) showing differentially expressed genes. Red, FDR ≤ 0.05 ; black, FDR > 0.05 . SCG, superior cervical ganglion.

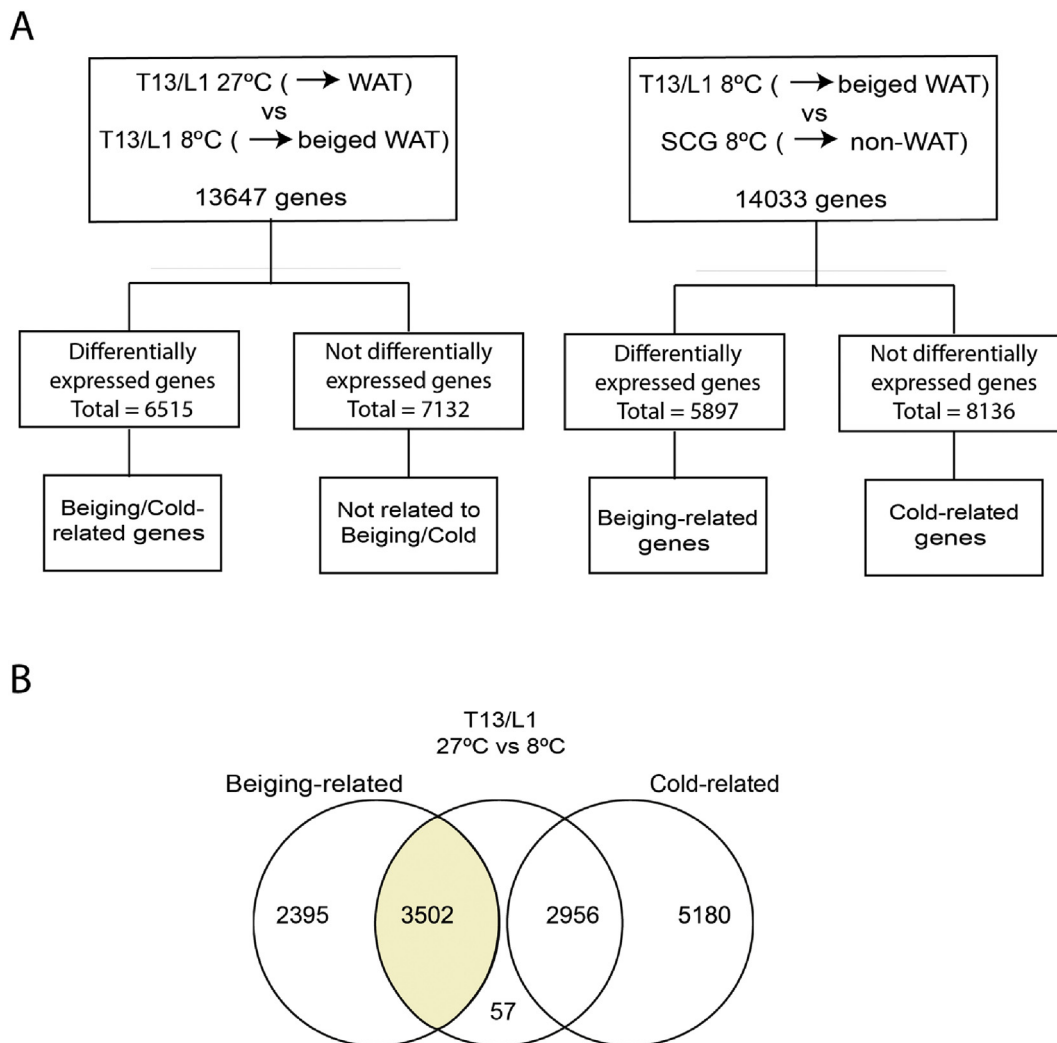


Figure 2: (A) Flow chart depicting RNA Sequencing analysis in T13/L1 ganglia at 27 °C and 8 °C and (B) T13/L1 ganglia and SCG at 8 °C. (B) Venn diagram demonstrating overlapping beiging- and cold-related genes in T13/L1 ganglia. Shaded area in (B) depicts the set of “beiging” related differentially expressed genes in T13/L1 ganglia.

beiging of iWAT (Figure 4A). Analysis of differentially expressed genes ($FDR \leq 0.05$) with respect to their relationship to specific diseases and biological functions revealed a substantial enrichment of processes related to the synthesis, oxidation and metabolism of lipids, carbohydrates, and amino acids (Figure 4B).

IPA also provides an exploratory analysis platform to predict upstream regulators where the activation or inhibition may explain the observed gene expression patterns. The basis of this analysis is that genes are assigned to upstream regulators based on previous experimental evidence from the literature. To investigate the possible molecular bases for the observed transcriptomic changes, we investigated the predicted upstream regulators of the list of differentially expressed genes ($P \leq 0.05$) within the T13/L1 ganglia that were related to the beiging of iWAT. The most significant predicted regulator was leptin ($P < 0.05$) with similarly important representation of the leptin receptor (Figure 4C). It is notable that in this leptin and leptin receptor network, there were a significant number of molecules from the dataset that have been defined as downstream targets. Of these overlapping molecules, the majority were upregulated (leptin: 17/18 and leptin receptor: 10/11) in response to the beiging of iWAT, suggesting an activation of these signaling pathway.

3.3.5. Analysis of impact of candidate neuropeptides on browning in cultured 3T3L1 adipocytes

In order to assess the impact of CGRP and α MSH on browning, we differentiated 3T3L1 preadipocytes into mature adipocytes, followed by treatment with the two candidate neuropeptides. Increasing concentrations of CGRP did not affect lipolysis (glycerol release) or the gene expression levels of *Ucp1*; however, treatment with α MSH resulted in a dose dependent elevation in gene expression, most pronounced at the highest concentration (10^{-7} M) (see Figure 5). Furthermore, assessment of another marker of browning, *Ppargc1*, also revealed a significant elevation following incubation with α MSH at the dose (10^{-7} M) that achieved maximal expression of *Ucp1*. In order to determine whether there was an interaction between stimulation of the beta-adrenergic receptor and treatment with the candidate peptides, cells were incubated with isoproterenol. Isoproterenol alone caused an increase in lipolysis and browning (*Ucp1* expression) following submaximal (10 nM) and maximal (10 μ M) stimulation. Co-incubation of CGRP or α MSH with a submaximal (10 nM) dose of isoproterenol did not modulate the impact of the two peptides on browning beyond what would be an indicative of an additive effect, as determined by *Ucp1* expression (data not shown).

Table 2 — Changes in gene expression in neuropeptides and neurotransmitters in T13/L1 ganglia after exposure to cold.

Gene	Gene Description	LogFC	FDR
Upregulated genes (LogFC ≥ 1)			
LOC500035	hypothetical protein LOC500035	10.07	4.74E-53
AC139642.2		5.23	1.32E-33
AABR07013776.1		8.75	3.80E-28
AC119603.1		6.33	8.37E-21
LOC680579	similar to ribosomal protein L14	3.84	7.86E-20
Gnal	G protein subunit alpha L	2.83	9.87E-18
RGD1564469	similar to Acidic ribosomal phosphoprotein P0	4.96	1.19E-17
RGD1563581	similar to S100 calcium binding protein A11 (calzarin)	2.10	1.56E-17
LOC100361920	dynein light chain 1-like	3.09	1.16E-15
Ucp1	uncoupling protein 1	8.03	2.08E-13
Dbp	D-box binding PAR bZIP transcription factor	3.16	2.79E-13
AABR07030494.1		3.55	3.63E-13
Fam111a	family with sequence similarity 111, member A	4.84	6.30E-13
Cidea	cell death-inducing DFFA-like effector a	6.28	2.28E-12
Tbca	tubulin folding cofactor A	3.14	2.53E-12
Cox8b	cytochrome c oxidase, subunit VIIIb	6.11	3.53E-12
Lag3	lymphocyte activating 3	4.28	5.17E-12
Gpr146	G protein-coupled receptor 146	2.75	2.39E-11
Cebpa	CCAAT/enhancer binding protein alpha	4.02	4.13E-11
Ybx3	Y box binding protein 2	4.26	4.64E-11
Downregulated genes (LogFC ≤ -1)			
RGD1562420	similar to hypothetical protein	-5.80	1.29E-33
Gm1141	predicted gene 1141	-6.19	2.06E-32
Ppia	peptidylprolyl isomerase A	-3.08	3.70E-32
LOC100359951	ribosomal protein S20-like	-7.38	5.73E-32
LOC690468	similar to 60S ribosomal protein L38	-8.29	8.47E-28
Rpl13	ribosomal protein L13	-3.99	4.87E-27
LOC689899	similar to 60S ribosomal protein L23a	-7.84	6.21E-27
LOC683961	similar to ribosomal protein S13	-6.00	1.67E-25
AABR07013410.1		-7.13	1.66E-21
RGD1564606	similar to 60S ribosomal protein L23a	-6.14	5.03E-19
LOC100364191	hCG1994130-like	-2.70	3.37E-18
Actg1	actin, gamma 1	-3.52	5.40E-17
Rpl37	ribosomal protein L37	-4.33	7.06E-17
AC136661.1		-3.88	8.32E-15
M6pr	cation-dependent mannose-6-phosphate receptor-like	-3.30	1.20E-14
AABR07068955.1		-3.79	1.81E-14
LOC108348118		-6.50	4.62E-14
RGD1564839	similar to ribosomal protein L31	-4.63	2.36E-13
Rfk	riboflavin kinase	-1.83	9.33E-13
Ankrd13c	ankyrin repeat domain 13C	-1.75	1.10E-12

4. DISCUSSION

These data indicate that with being of iWAT, there is a coincident shift in the gene expression profile of neurons in paravertebral ganglia projecting to this adipose tissue pad. Significantly, this pattern of gene expression becomes more aligned with that of neurons projecting to BAT rather than to WAT. Of the biosynthetic pathways and individual genes coding for known neurotransmitters and neuropeptides that are enhanced in their expression in ganglionic neurons following cold-induced being, POMC and CGRP emerge as prime candidates. Of these, POMC is shown to induce the expression of brown-like or beige gene markers in cultured adipocytes.

The extended autonomic neuraxis providing the innervation of peripheral tissues via sympathetic preganglionic neurons projecting to the SCG (head and neck), stellate ganglion (predominantly brown fat,

heart and trachea), and T13/L1 ganglia (inguinal fat) is illustrated in [Supplementary Figure 2](#). Essentially, this is comprised of “premotor” neurons in the brain stem and hypothalamus, sympathetic preganglionic neurons in the thoracolumbar spinal cord, and ganglionic neurons housed in the ganglia noted above.

In addition to these major topographical divisions, the present studies are based on the premise that there is a basic neurochemical code that exists in neurons of the paravertebral ganglia and other parts of sympathetic outflow to particular endpoints that is characteristic of that end organ. A corollary of this fact is that with the changing structure and function of iWAT that occurs with browning in response to cold or other stimuli, there is (necessarily) a reorganization of the nervous system, including sympathetic postganglionic neurons to accommodate that change and facilitate the coordinated physiological recruitment of the new “brown-like” phenotype of iWAT.

The notion that a “chemical code” [24] or “neurochemical signature” [25] exists in postganglionic and even preganglionic sympathetic neurons is not new (for review see [22]). In fact, the idea that a combination of transmitters, modulators, receptors, or intracellular signaling entities form a code that might be unique to a functional class of neurons has driven, and continues to drive, a number of studies of regions deeper in the autonomic neuraxis, particularly in the hypothalamus. It seems likely, however, that the association between a chemical signature and a functional endpoint is most robust in those parts of the nervous system closest the endpoint, namely the postganglionic neuron and as such “upstream populations” including preganglionic neurons were not assessed for gene changes. Postganglionic neurons, for example, projecting directly to salivary glands are noradrenergic and enkephalinergic [36–38], whereas those sudomotor inputs to sweat glands are uniquely cholinergic and vasoactive intestinal peptide and CGRP-containing [39,40]. While these few examples and those noted in the Introduction are part of a compendium of codes, the broader question of whether the chemical phenotype of postganglionic neurons is predetermined and directs axons during development to seek out a specific end tissue (target independent), or conversely, whether target tissues induce a ganglionic neuron to adopt an “appropriate” chemical phenotype (target dependent differentiation), remains unresolved. Certainly, the last attempt to summarize the evidence supporting either of these propositions was inconclusive [22]. Importantly, the present RNA-seq data, which show a dramatic shift in gene expression profiles from 24% differentially expressed genes in the T13/L1 ganglia at thermoneutrality between iWAT and iBAT to just 5% after cold exposure and browning of iWAT, are consistent with a primary role of the target tissue in the determination of neurochemical phenotype. More relevant to the question in this study, these data begin to define a phenotype that is related to the browning of WAT. In this respect, it has been assumed throughout these analyses that the neurons best representing the paravertebral ganglionic input to iBAT are those in the stellate ganglion. While this is true, it should also be recognized that there is input to iBAT from adjacent ganglia in the upper thoracic sympathetic chain, namely from T3–T5 [35]. It should also be recognized that while the gene changes associated with cold exposure in the stellate ganglion are likely a reflection of the input of stellate ganglionic neurons to the iBAT, neurons in the ganglion also project to the heart and trachea. The implication of this is that the magnitude of the gene changes is likely to be underestimated given the presence of neurons that are less likely to respond to the stimulus.

The premise that there must be some reorganization of neural pathways after being of iWAT is supported indirectly by studies showing that it can be functionally recruited to promote better metabolic

Table 3 — Changes in neuropeptides and neurotransmitters in T13/L1 ganglia after exposure to cold.

Neuropeptide	Gene Symbol	Name of genes	LogFC	FDR
Calcitonin Gene Related Peptide (CGRP)	Calca	Calcitonin-Related Polypeptide Alpha	2.03	6.93E-04
Enkephalin (ENK)	Pomc	Proopiomelanocortin	1.48	3.91E-03
	Penk	Proenkephalin	1.90	1.56E-03
Noradrenaline	Th	Tyrosine Hydroxylase	0.89	5.79E-04
	Dbh	Dopamine Beta-Hydroxylase	-0.29	2.76E-01
	Ddc	Dopa Decarboxylase (Aromatic L-Amino Acid Decarboxylase)	-0.79	3.15E-03
	^a Qdpr	Quinoid Dihydropteridine Reductase	-0.31	2.37E-01
Substance P	^a Tac1	Tachykinin, Precursor 1	1.93	5.16E-03
Vasoactive Intestinal Peptide	VIP	Vasoactive Intestinal Peptide	-0.22	6.81E-01
Neuropeptide Y	Npy	Neuropeptide Y	not detected	not detected
Calretinin (CALRET)	Calb1	Calbindin 1	-0.29	4.84E-01
Glutamate	Gad1	Glutamate Decarboxylase 1	not detected	not detected
Nitric Oxide	^a Nos1	Nitric Oxide Synthase 1 (Neuronal)	1.08	2.5E-02
Acetylcholine	Ache	Acetylcholinesterase	0.69	1.02E-03
	Chat	Choline Acetyltransferase	1.45	9.46E-03
Pituitary Adenylate Cyclase-Activating Peptide (PACAP)	Adcyap1	Adenylate Cyclase Activating Polypeptide 1	not detected	not detected

^a Designates cold-related gene i.e. similar expression between T13/L1 and SCG at 8 °C.

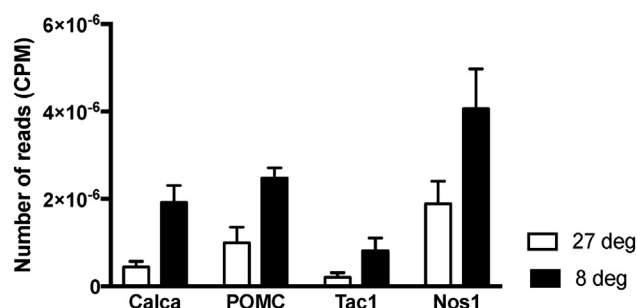


Figure 3: Number of reads (CPM) of CGRP (*Calca*), POMC (*Pomc*), Substance P (*Tac1*) and Nitric Oxide Synthase 1 (*Nos1*) following RNA Sequencing T13/L1 ganglia at 27 °C and 8 °C.

outcomes in rodent models and humans (for review, see [41]). In other words, despite the transition from an adipose tissue pad that is primarily involved in lipid storage to one that contributes significantly to energy expenditure [42] and, after transformation, is driven by the sensory modalities of temperature and diet rather than stimuli that promote lipolysis, beigned iWAT is activated in a physiologically meaningful way. The weight of evidence suggests that this must involve central integrated neural circuits [43,44]. In fact, a recent viral tracing study indicates that, coincident with the beiging of iWAT, there

are changes in discrete supraspinal brain regions [45], which, together with the shifts in gene expression in post ganglionic neurons described here, support the thesis that the beiging of WAT involves a coordinated response in the nervous system and targeted adipose tissue depot. The strategy employed in the present study involved a comparison of RNA-Seq generated data from T13/L1 (to iWAT) and stellate (to iBAT) ganglia after cold exposure with gene expression profiles in the SCG, which has no substantial projection to WAT, that, taken together, increases the likelihood of defining changes that are related to beiging rather than to cold exposure itself. Analysis of a set of “beiging” related genes provided a list of up- and down-regulated genes that predominantly have structural or ribosomal functions, or, in many cases, do not have a previously described function. Further assessment using IPA enabled a more refined analysis, integration, and understanding of the gene expression data following RNA-Seq in the context of canonical pathways and specific diseases and functions. In this respect, the top ranked canonical pathways were related to mitochondrial function (mitochondrial function and sirtuin signalling) and substrate metabolism (oxidative phosphorylation and fatty acid oxidation). In the same vein, assessment of beiging related genes with respect to diseases or functions indicated an enrichment of genes involved in synthesis, metabolism, and/or oxidation of carbohydrates, fatty acids, and amino acids. Given that the maintenance of neuronal activity is critically dependent on an adequate energy supply, which functions to regulate

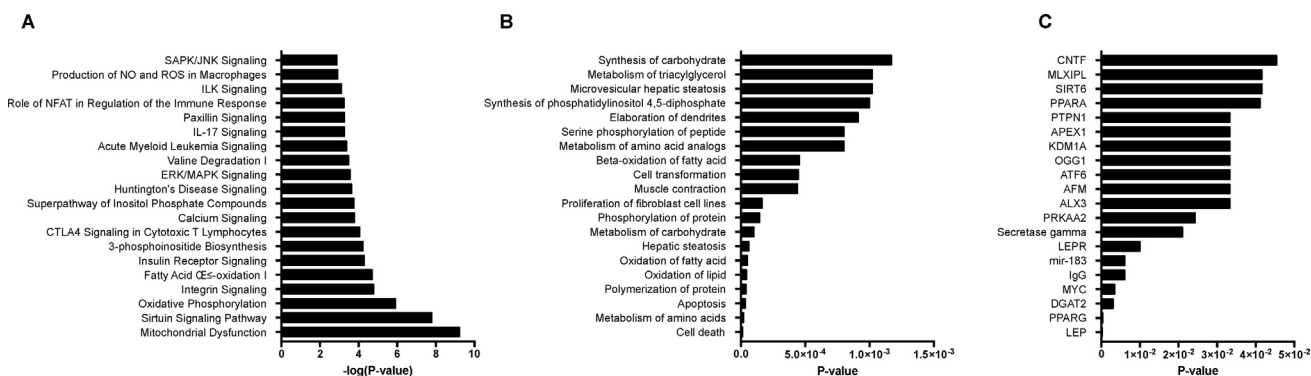


Figure 4: Classification of differentially expressed genes in the T13/L1 ganglia that are associated with the beiging of iWAT according to the top twenty (A) canonical pathways, (B) diseases and functions, and (C) predicted upstream regulators. Bars in (A) indicate the likelihood [$-\log(P\text{-value})$] that the specific pathway is implicated in regulating the beiging of iWAT and the p-value of overlap of molecules detected in dataset with those associated with specific (B) diseases and functions and (C) upstream regulators.

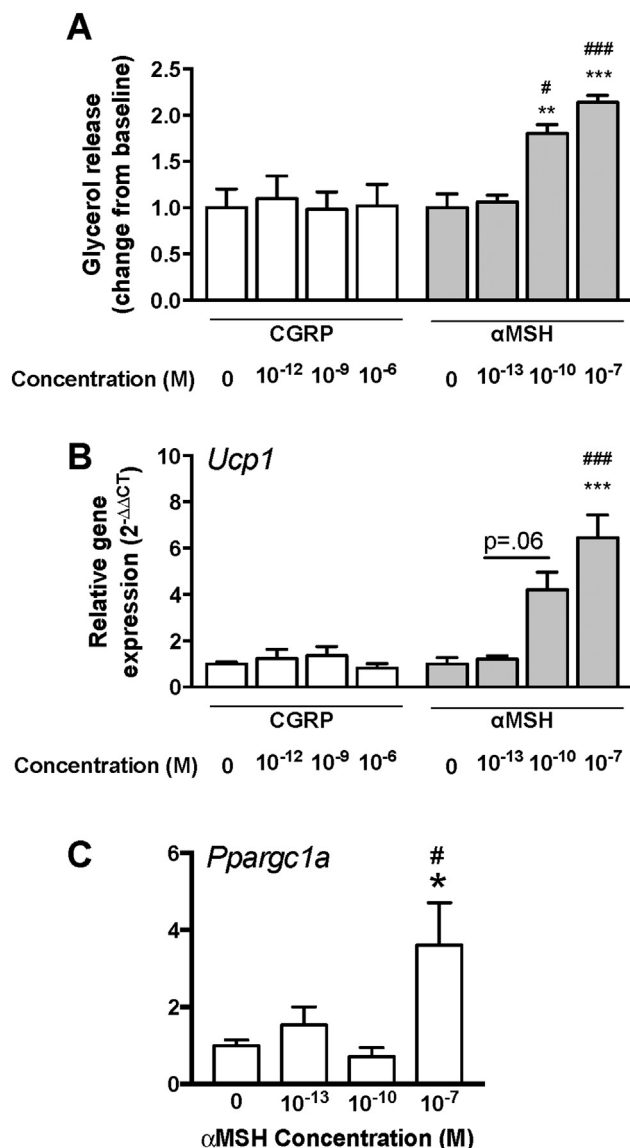


Figure 5: (A) Glycerol release (change from baseline), (B) *Ucp1* and (C) *Ppargc1a* gene expression in 3T3L1 adipocytes following treatment (6 h) with candidate neuropeptides, CGRP (0, 10^{-12} , 10^{-9} , 10^{-6} M) and/or α MSH (0, 10^{-13} , 10^{-10} , 10^{-7} M). * $P < .05$, compared to α MSH (0); # $P < .05$, compared α MSH (10^{-13} M), *** $P < .0001$, compared to α MSH (0); ### $P < .0001$, compared α MSH (10^{-13} M).

pre- and post-synaptic action potentials, transmitter release, and post-synaptic currents [46], it is not surprising that there is an upregulation of processes that will ultimately lead to the generation of ATP from oxidative phosphorylation.

Assessment of predicted upstream regulators demonstrated leptin as the most likely candidate molecule to explain the observed gene expression profiles. Leptin has an undeniable role in the regulation of energy homeostasis; however, this is primarily based on evidence derived from its function in the hypothalamus, including the arcuate nucleus [for review, see [47]]. There is accumulating evidence that, besides its involvement in appetite regulation, the arcuate nucleus also regulates thermogenic activity. For example, viral tracing studies have established that leptin receptor expressing neurons in the arcuate nucleus are polysynaptically connected to BAT [29], and leptin administration into the arcuate nucleus results in an elevation in

sympathetic drive to BAT [48], whereas deletion of leptin signaling in the arcuate nucleus abolishes sympathetic activation of BAT [49]. The interaction between leptin and the autonomic nervous system was further corroborated in a recent study which demonstrated the leptin-induced lipolysis in WAT is directly mediated by sympathetic neurons that innervate white adipocytes [43]. Importantly, in the context of the current findings that beige adipose tissue is associated with a coincident shift in neuropeptide gene expression, this recent study suggests that the leptin-induced production of noradrenaline from sympathetic neurons could act through additional receptors (i.e. non β -adrenergic receptors) and highlights the possibility that sympathetic post-ganglionic neurons may co-release other neurotransmitters and neuropeptides that signal through non-adrenergic receptors.

The upregulation of *Pomc* in the targeted gene analysis is consistent with the well-established function of POMC, or more specifically peptides cleaved from this protein, in the regulation of energy balance [50]. In this respect, we and others have shown that manipulation of melanocortin receptor signaling, either via central administration of α MSH, a POMC-derived peptide, or the melanocortin receptor antagonist SHU9119, results in a shift in BAT activity [51–53]. In addition, the involvement of POMC neurons in the regulation of thermogenesis was also recently shown to be dependent on the function of phosphatases within these neurons (PTP1B and TCPTP) and co-administration of leptin and insulin to mice exerts a synergistic effect by the promotion of browning in iWAT [54]. Consistent with a role of POMC products in the beiging process, albeit by a peripheral mechanism, is the recent observation that methionine-enkephalin peptides released from group 2 innate lymphoid cells can act directly on adipocytes to upregulate *Ucp1* expression *in vitro* and promote beiging in iWAT with a corresponding shift in oxygen consumption *in vivo* [55]. To our knowledge, however, ours is the first report of POMC processing in paravertebral ganglia. This combined with the present result of α MSH induced expression of UCP1 and PCG1 α in cultured 3T3L1 adipocytes, highlights the potential for a direct action of POMC products on inguinal WAT to promote browning.

The targeted gene analysis also demonstrated a significant upregulation of CGRP and Substance P, the latter of which occurred as a generalized response to cold. In addition, TH was also elevated after cold exposure, consistent with the sprouting of (presumably) noradrenergic fibers amongst newly formed beige adipocytes in the iWAT, an observation made in a previous study [45] and in a number of different visceral and subcutaneous adipose tissue depots [56]. CGRP and SP-containing nerve fibers are present within peri-ovarian WAT, and their density is increased in the vicinity of brown-like transformed adipocytes after cold exposure [57]. Much of this increase in fiber density was reversed by capsaicin treatment, consistent with a proportion of these being sensory in nature [57], a result which is not surprising given the widespread representation of both peptide transmitters in sensory projections. Consistent with capsaicin treatment in peri-ovarian adipose tissue depots, epididymal WAT shows a reduction in CGRP-containing nerve fibers, but no significant decrease in TH-containing nerve fibers after capsaicin treatment [58]. However, after surgical denervation of epididymal WAT, which necessarily involves separation of both sympathetic and sensory fibres from the adipose tissue pad, there is a greater reduction in the number of CGRP-containing nerve fibers compared to only the elimination of sensory fibers, and a similar decrease in TH-containing fibers [58]. The reduction in TH-containing nerve fibers and the further reduction in CGRP-positive fibers suggests a role for CGRP in sympathetic input. The simplest explanation of these data from others and those from the present experiments is that the population of CGRP fibers in iWAT includes those with parent cell bodies in both the dorsal root ganglia (sensory) and the T13/L1 ganglia

(sympathetic). In fact, CGRP mRNA is present in T13/L1 ganglia as demonstrated with hybridization histochemistry (data not shown). Intriguingly, UCP1, the enzyme responsible for uncoupling oxidative phosphorylation in BAT and, CIDEA, a lipid droplet protein enriched in brown adipocyte, are both elevated in T13/L1 ganglia. While the upregulation of neuronal *Ucp1* and *Cidea* is interesting and more specifically, their association with the beiging process is “eye-catching”, their function is more likely to reflect the cold stimulus used to induce the beiging process. Further evidence for the involvement of UCP1 in response to cold exposure is derived from studies in torpid mammals (ground squirrels), in which, coincident with reduced body temperatures during hibernation, there is an increase in functional UCP1 protein within both the cortex and dorsal root ganglia [59]. Similarly, carp, a non-mammalian species, have also been shown to have increased UCP1 within brain regions after cold acclimation [60]. These observations are consistent with the idea that mammalian hibernators and other non-hibernating species are able to use neuronal UCP1 to supply heat, aiding in the maintenance of the basal activity of both the central and peripheral nervous systems during exposure to cold or low metabolic activity.

Taken together, these data demonstrate that there is a significant shift in the gene expression profile in neurons directly innervating iWAT, concomitant with the beiging process, to a signature which is more aligned with that of neurons innervating iBAT. Among the genes that are changed that may modulate the beiging process are those coding for POMC and CGRP, and, of these, based on *in vitro* experiments, POMC, or specifically, its cleavage product α MSH, appears to be the most viable candidate contributing to the process. This represents the first direct insight into the nature of the innervation of beige adipocytes and supports the long-held and general notion that ganglionic neurons contain a neurochemical signature that relates them directly to the structures that they innervate. The results are also consistent with a recently identified central reorganization that occurs coincident with the browning of iWAT. Both the changes in central integrative neural pathways and gene expression in peripheral ganglia provide a basis for the functional recruitment of beighed white adipocytes.

DECLARATION OF INTEREST

This work is supported by a grant from the NHMRC Australia (APP1082599) and a NHMRC Fellowship to BJO (APP1022451) and MJW (APP1077703).

CONFLICT OF INTEREST

None declared.

APPENDIX A. SUPPLEMENTARY DATA

Supplementary data related to this article can be found at <https://doi.org/10.1016/j.molmet.2018.01.024>.

REFERENCES

- [1] Hany, T.F., Gharehpapagh, E., Kamel, E.M., Buck, A., Himms-Hagen, J., von Schulthess, G.K., 2002. Brown adipose tissue: a factor to consider in symmetrical tracer uptake in the neck and upper chest region. *European Journal of Nuclear Medicine and Molecular Imaging* 29(10):1393–1398.
- [2] Cohade, C., Mourtzikos, K.A., Wahl, R.L., 2003. “USA-Fat”: prevalence is related to ambient outdoor temperature-evaluation with 18F-FDG PET/CT. *Journal of Nuclear Medicine* 44(8):1267–1270.
- [3] Nedergaard, J., Bengtsson, T., Cannon, B., 2007. Unexpected evidence for active brown adipose tissue in adult humans. *American Journal of Physiology. Endocrinology and Metabolism* 293(2):E444–E452.
- [4] van Marken Lichtenbelt, W.D., Vanhommerig, J.W., Smulders, N.M., Drossaerts, J.M., Kemerink, G.J., Bouvy, N.D., et al., 2009. Cold-activated brown adipose tissue in healthy men. *New England Journal of Medicine* 360(15):1500–1508.
- [5] Virtanen, K.A., Lidell, M.E., Orava, J., Heglind, M., Westergren, R., Niemi, T., et al., 2009. Functional brown adipose tissue in healthy adults. *New England Journal of Medicine* 360(15):1518–1525.
- [6] Cypess, A.M., Lehman, S., Williams, G., Tal, I., Rodman, D., Goldfine, A.B., et al., 2009. Identification and importance of brown adipose tissue in adult humans. *New England Journal of Medicine* 360(15):1509–1517.
- [7] Petrovic, N., Walden, T.B., Shabalina, I.G., Timmons, J.A., Cannon, B., Nedergaard, J., 2010. Chronic peroxisome proliferator-activated receptor gamma (PPARgamma) activation of epididymally derived white adipocyte cultures reveals a population of thermogenically competent, UCP1-containing adipocytes molecularly distinct from classic brown adipocytes. *Journal of Biological Chemistry* 285(10):7153–7164.
- [8] Ishibashi, J., Seale, P., 2010. Medicine. Beige can be slimming. *Science* 328(5982):1113–1114.
- [9] Wu, J., Bostrom, P., Sparks, L.M., Ye, L., Choi, J.H., Giang, A.H., et al., 2012. Beige adipocytes are a distinct type of thermogenic fat cell in mouse and human. *Cell* 150(2):366–376.
- [10] Rosenwald, M., Perdikari, A., Rulicke, T., Wolfrum, C., 2013. Bi-directional interconversion of brite and white adipocytes. *Nature Cell Biology* 15(6):659–667.
- [11] Wang, Q.A., Tao, C., Gupta, R.K., Scherer, P.E., 2013. Tracking adipogenesis during white adipose tissue development, expansion and regeneration. *Nature Medicine* 19(10):1338–1344.
- [12] Xue, R., Lynes, M.D., Dreyfuss, J.M., Shamsi, F., Schulz, T.J., Zhang, H., et al., 2015. Clonal analyses and gene profiling identify genetic biomarkers of the thermogenic potential of human brown and white preadipocytes. *Nature Medicine* 21(7):760–768.
- [13] Nyman, E., Bartesaghi, S., Melin Rydfalk, R., Eng, S., Pollard, C., Gennemark, P., et al., 2017. Systems biology reveals uncoupling beyond UCP1 in human white fat-derived beige adipocytes. *NPJ Systems Biology and Applications*, 329.
- [14] Shinoda, K., Luijten, I.H., Hasegawa, Y., Hong, H., Sonne, S.B., Kim, M., et al., 2015. Genetic and functional characterization of clonally derived adult human brown adipocytes. *Nature Medicine* 21(4):389–394.
- [15] Jespersen, N.Z., Larsen, T.J., Peijs, L., Dagaard, S., Homoe, P., Loft, A., et al., 2013. A classical brown adipose tissue mRNA signature partly overlaps with brite in the supraclavicular region of adult humans. *Cell Metabolism* 17(5):798–805.
- [16] Cypess, A.M., White, A.P., Vernochet, C., Schulz, T.J., Xue, R., Sass, C.A., et al., 2013. Anatomical localization, gene expression profiling and functional characterization of adult human neck brown fat. *Nature Medicine* 19(5):635–639.
- [17] Lee, P., Swarbrick, M.M., Zhao, J.T., Ho, K.K., 2011. Inducible brown adipogenesis of supraclavicular fat in adult humans. *Endocrinology* 152(10):3597–3602.
- [18] Sidossis, L.S., Porter, C., Saraf, M.K., Borsheim, E., Radhakrishnan, R.S., Chao, T., et al., 2015. Browning of subcutaneous white adipose tissue in humans after severe adrenergic stress. *Cell Metabolism* 22(2):219–227.
- [19] Seale, P., Conroe, H.M., Estall, J., Kajimura, S., Frontini, A., Ishibashi, J., et al., 2011. Prdm16 determines the thermogenic program of subcutaneous white adipose tissue in mice. *Journal of Clinical Investigation* 121(1):96–105.
- [20] Cohen, P., Levy, J.D., Zhang, Y., Frontini, A., Kolodin, D.P., Svensson, K.J., et al., 2014. Ablation of PRDM16 and beige adipose causes metabolic dysfunction and a subcutaneous to visceral fat switch. *Cell* 156(1–2):304–316.
- [21] Min, S.Y., Kady, J., Nam, M., Rojas-Rodriguez, R., Berkenwald, A., Kim, J.H., et al., 2016. Human ‘brite/beige’ adipocytes develop from capillary networks,

- and their implantation improves metabolic homeostasis in mice. *Nature Medicine* 22(3):312–318.
- [22] Cane, K.N., Anderson, C.R., 2009. Generating diversity: mechanisms regulating the differentiation of autonomic neuron phenotypes. *Autonomic Neuroscience* 151(1):17–29.
- [23] Macrae, I.M., Furness, J.B., Costa, M., 1986. Distribution of subgroups of noradrenaline neurons in the coeliac ganglion of the Guinea-pig. *Cell and Tissue Research* 244(1):173–180.
- [24] Furness, J.B., Morris, J.L., Gibbins, I.L., Costa, M., 1989. Chemical coding of neurons and plurichemical transmission. *Annual Review of Pharmacology and Toxicology*, 29289–29306.
- [25] Lam, D.M., Li, H.B., Su, Y.Y., Watt, C.B., 1985. The signature hypothesis: colocalizations of neuroactive substances as anatomical probes for circuitry analyses. *Vision Research* 25(10):1353–1364.
- [26] Apostolova, G., Dorn, R., Ka, S., Hallbook, F., Lundeberg, J., Liser, K., et al., 2007. Neurotransmitter phenotype-specific expression changes in developing sympathetic neurons. *Molecular and Cellular Neuroscience* 35(3):397–408.
- [27] Apostolova, G., Dechant, G., 2009. Development of neurotransmitter phenotypes in sympathetic neurons. *Autonomic Neuroscience* 151(1):30–38.
- [28] Grkovic, I., Anderson, C.R., 1997. Calbindin D28K-immunoreactivity identifies distinct subpopulations of sympathetic pre- and postganglionic neurons in the rat. *The Journal of Comparative Neurology* 386(2):245–259.
- [29] Oldfield, B.J., Giles, M.E., Watson, A., Anderson, C., Colvill, L.M., McKinley, M.J., 2002. The neurochemical characterisation of hypothalamic pathways projecting polysynaptically to brown adipose tissue in the rat. *Neuroscience* 110(3):515–526.
- [30] Dobin, A., Davis, C.A., Schlesinger, F., Drenkow, J., Zaleski, C., Jha, S., et al., 2013. STAR: ultrafast universal RNA-seq aligner. *Bioinformatics* 29(1):15–21.
- [31] Liao, Y., Smyth, G.K., Shi, W., 2014. featureCounts: an efficient general purpose program for assigning sequence reads to genomic features. *Bioinformatics* 30(7):923–930.
- [32] Ewels, P., Magnusson, M., Lundin, S., Kaller, M., 2016. MultiQC: summarize analysis results for multiple tools and samples in a single report. *Bioinformatics* 32(19):3047–3048.
- [33] Robinson, M.D., McCarthy, D.J., Smyth, G.K., 2010. edgeR: a Bioconductor package for differential expression analysis of digital gene expression data. *Bioinformatics* 26(1):139–140.
- [34] Risso, D., Ngai, J., Speed, T.P., Dudoit, S., 2014. Normalization of RNA-seq data using factor analysis of control genes or samples. *Nature Biotechnology* 32(9):896–902.
- [35] Jansen, A.S., Nguyen, X.V., Karpitskiy, V., Mettenleiter, T.C., Loewy, A.D., 1995. Central command neurons of the sympathetic nervous system: basis of the fight-or-flight response. *Science* 270(5236):644–646.
- [36] Shida, T., Ueda, Y., Ishida-Yamamoto, A., Senba, E., Tohyama, M., 1991. Enkephalinergic sympathetic and parasympathetic innervation of the rat submandibular and sublingual glands. *Brain Research* 555(2):288–294.
- [37] Soinila, J., Happola, O., Yanaihara, N., Soinila, S., 1991. Immunohistochemical localization of [Met5]enkephalin and [Met5]enkephalin-Arg6-Gly7-Leu8 in sympathetic and parasympathetic neurons and nerve fibers projecting to the rat submandibular gland. *Neuroscience* 40(2):545–554.
- [38] Soinila, J., Salo, A., Uusitalo, H., Soinila, S., Yanaihara, N., Happola, O., 1991. Met5-enkephalin-Arg6-Gly7-Leu8-immunoreactive nerve fibers in the major salivary glands of the rat: evidence for both sympathetic and parasympathetic origin. *Cell and Tissue Research* 264(1):15–22.
- [39] Heym, C., Liu, N., Gleich, A., Oberst, P., Kummer, W., 1993. Immunohistochemical evidence for different pathways immunoreactive to substance P and calcitonin gene-related peptide (CGRP) in the Guinea-pig stellate ganglion. *Cell and Tissue Research* 272(3):563–574.
- [40] Leblanc, G., Landis, S., 1986. Development of choline acetyltransferase (CAT) in the sympathetic innervation of rat sweat glands. *Journal of Neuroscience* 6(1):260–265.
- [41] Kajimura, S., Spiegelman, B.M., Brown, Seale P., Fat, Beige, 2015. Physiological roles beyond heat generation. *Cell Metabolism* 22(4):546–559.
- [42] Dodd, G.T., Andrews, Z.B., Simonds, S.E., Michael, N.J., DeVeer, M., Bruning, J.C., et al., 2017. A hypothalamic phosphatase switch coordinates energy expenditure with feeding. *Cell Metabolism* 26(3):577.
- [43] Zeng, W., Pirzalska, R.M., Pereira, M.M., Kubasova, N., Barateiro, A., Seixas, E., et al., 2015. Sympathetic neuro-adipose connections mediate leptin-driven lipolysis. *Cell* 163(1):84–94.
- [44] Fischer, K., Ruiz, H.H., Jhun, K., Finan, B., Oberlin, D.J., van der Heide, V., et al., 2017. Alternatively activated macrophages do not synthesize catecholamines or contribute to adipose tissue adaptive thermogenesis. *Nature Medicine* 23(5):623–630.
- [45] Wiedmann, N.M., Stefanidis, A., Oldfield, B.J., 2017. Characterization of the central neural projections to brown, white, and beige adipose tissue. *The FASEB Journal* 31(11):4879–4890.
- [46] Hall, C.N., Klein-Flugge, M.C., Howarth, C., Attwell, D., 2012. Oxidative phosphorylation, not glycolysis, powers presynaptic and postsynaptic mechanisms underlying brain information processing. *Journal of Neuroscience* 32(26):8940–8951.
- [47] Pandit, R., Beerens, S., Adan, R.A.H., 2017. Role of leptin in energy expenditure: the hypothalamic perspective. *American Journal of Physiology - Regulatory, Integrative and Comparative Physiology* 312(6):R938–R947.
- [48] Rahmouni, K., Morgan, D.A., 2007. Hypothalamic arcuate nucleus mediates the sympathetic and arterial pressure responses to leptin. *Hypertension* 49(3):647–652.
- [49] Harlan, S.M., Morgan, D.A., Agassandian, K., Guo, D.F., Cassell, M.D., Sigmund, C.D., et al., 2011. Ablation of the leptin receptor in the hypothalamic arcuate nucleus abrogates leptin-induced sympathetic activation. *Circulation Research* 108(7):808–812.
- [50] Myers, M.G., Cowley, M.A., Munzberg, H., 2008. Mechanisms of leptin action and leptin resistance. *Annual Review of Physiology*, 70537–70556.
- [51] Verty, A.N., Allen, A.M., Oldfield, B.J., 2010. The endogenous actions of hypothalamic peptides on brown adipose tissue thermogenesis in the rat. *Endocrinology* 151(9):4236–4246.
- [52] Yasuda, T., Masaki, T., Sakata, T., Yoshimatsu, H., 2004. Hypothalamic neuronal histamine regulates sympathetic nerve activity and expression of uncoupling protein 1 mRNA in brown adipose tissue in rats. *Neuroscience* 125(3):535–540.
- [53] Yasuda, T., Masaki, T., Kakuma, T., Yoshimatsu, H., 2004. Hypothalamic melanocortin system regulates sympathetic nerve activity in brown adipose tissue. *Experimental Biology and Medicine (Maywood)* 229(3):235–239.
- [54] Dodd, G.T., Decherf, S., Loh, K., Simonds, S.E., Wiede, F., Bolland, E., et al., 2015. Leptin and insulin act on POMC neurons to promote the browning of white fat. *Cell* 160(1–2):88–104.
- [55] Brestoff, J.R., Kim, B.S., Saenz, S.A., Stine, R.R., Monticelli, L.A., Sonnenberg, G.F., et al., 2015. Group 2 innate lymphoid cells promote beiging of white adipose tissue and limit obesity. *Nature* 519(7542):242–246.
- [56] Murano, I., Barbatelli, G., Giordano, A., Cinti, S., 2009. Noradrenergic parasympathetic nerve fiber branching after cold acclimatization correlates with brown adipocyte density in mouse adipose organ. *Journal of Anatomy* 214(1):171–178.
- [57] Giordano, A., Morroni, M., Santone, G., Marchesi, G.F., Cinti, S., 1996. Tyrosine hydroxylase, neuropeptide Y, substance P, calcitonin gene-related peptide and vasoactive intestinal peptide in nerves of rat periovarian adipose tissue: an immunohistochemical and ultrastructural investigation. *Journal of Neurocytology* 25(2):125–136.
- [58] Shi, H., Bartness, T.J., 2005. White adipose tissue sensory nerve denervation mimics lipectomy-induced compensatory increases in adiposity. *American Journal of Physiology - Regulatory, Integrative and Comparative Physiology* 289(2):R514–R520.

- [59] Laursen, W.J., Mastrotto, M., Pesta, D., Funk, O.H., Goodman, J.B., Merriman, D.K., et al., 2015. Neuronal UCP1 expression suggests a mechanism for local thermogenesis during hibernation. *Proceedings of the National Academy of Sciences of the U S A* 112(5):1607–1612.
- [60] Jastroch, M., Buckingham, J.A., Helwig, M., Klingenspor, M., Brand, M.D., 2007. Functional characterisation of UCP1 in the common carp: uncoupling activity in liver mitochondria and cold-induced expression in the brain. *Journal of Comparative Physiology B* 177(7):743–752.